Supporting Information.

Hollow core-shell heterojunction TAPB-COF@$ZnIn_2S_4$ as high efficient photocatalysts for carbon dioxide reduction

Huitao Fan*, Minglin Hu, Yabing Duan, Luyang Zuo, Ronggui Yu, Zhuwei Li, Qi Liu, Bo Li*, Liya Wang

College of Chemistry and Pharmaceutical Engineering, Nanyang Normal University, Nanyang, 473601, P. R. China

Corresponding Authors

*E-mail address: fanhuitao818@nynu.edu.cn (Huitao Fan), libony0107@nynu.edu.cn (Bo Li)

1. Characterizations

The apparent quantum yield (AQY)

The apparent quantum yield (AQY) was measured using different monochromatic light filters (380, 400, 420 nm), and the power meter (PL-MW 2000 photoradiometer, Perfect Light) was used to measure the number of incident photons.

$$AQY = \frac{Ne}{Np} \times 100\% = \frac{10^9 \times v \times N_A \times k \times h \times c}{I \times A \times \lambda} \times 100\%$$

Where, Ne is the number of reacted electrons, Np is the number of used photons, v is the reaction rate (mol s^{-1}), N_A is Avogadro constant, k is number of electrons transferred by the reaction, h is the Planck constant, c is the speed of light, I is the light intensity (W m^{-2}), A is the irradiation area, λ is the wavelength of incident light.

The TRPL

The TRPL spectra are both fitted with the bi-exponential decay function $y = A_1 e^{-t/\tau_2} + A_2 e^{-t/\tau_2}$, where τ_1 is the fast-decay component, τ_2 is the slow-decay component, A_1 and A_2 are the corresponding amplitudes. The average lifetime (Ave.τ) is calculated by

$$Ave.\tau = \frac{A_1\tau_1^2 + A_2\tau_2^2}{A_1\tau_1 + A_2\tau_2}$$

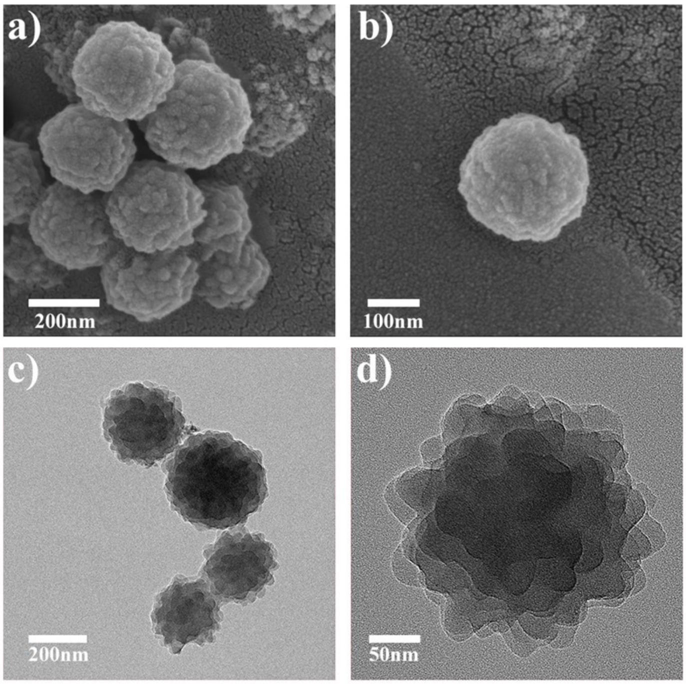

Fig. S1 a, b) FESEM images, c, d) TEM images of TAPB-DVA.

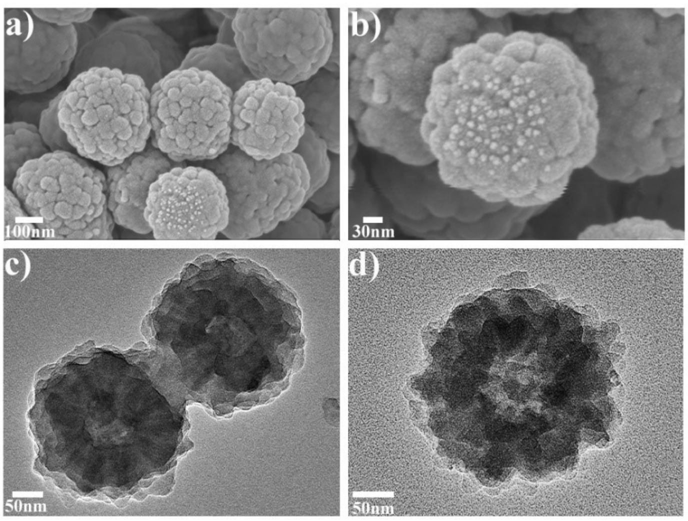

Fig. S2 a, b) FESEM images, c, d) TEM images of TAPB-COF.

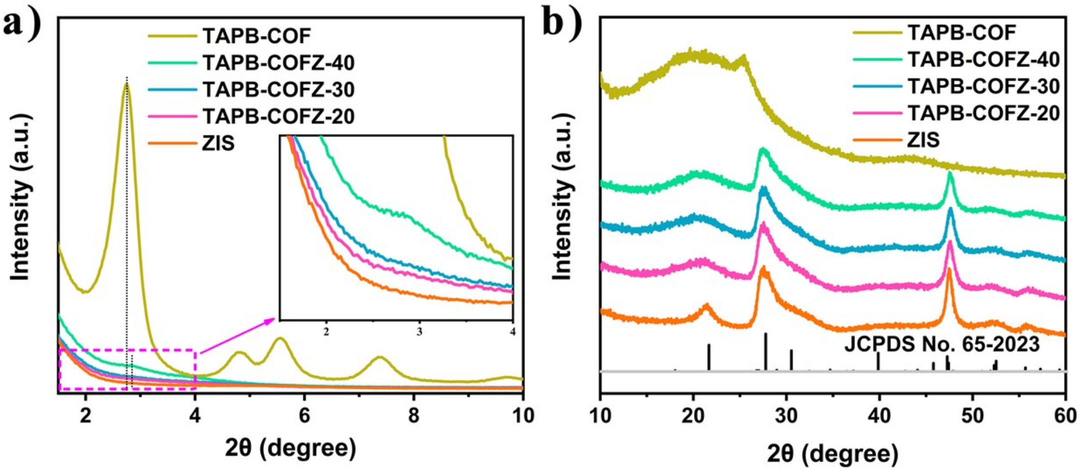

Fig. S3 a, b) PXRD pattern of ZIS, TAPB-COF, and TAPB-COFZ-x (x = 20, 30, 40).

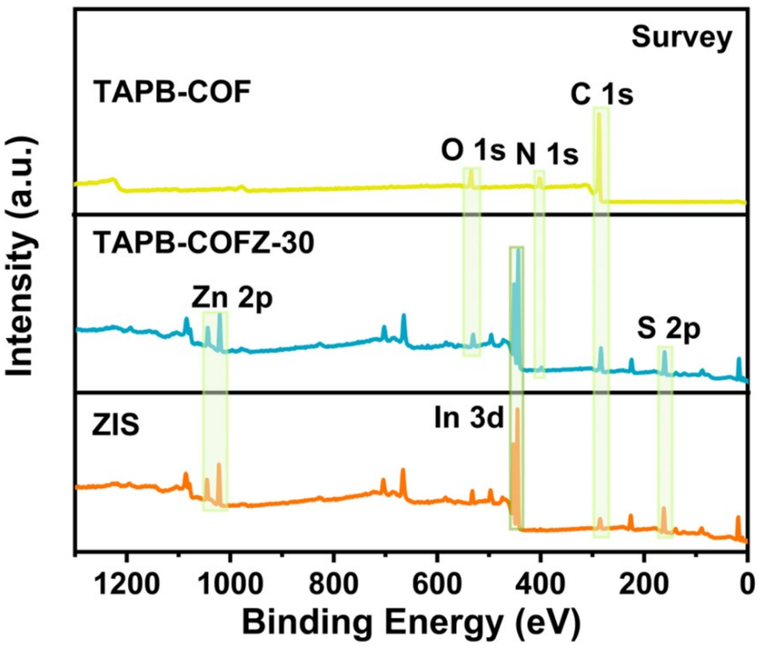

Fig. S4 XPS survey spectra of ZIS, TAPB-COF and TAPB-COFZ-30.

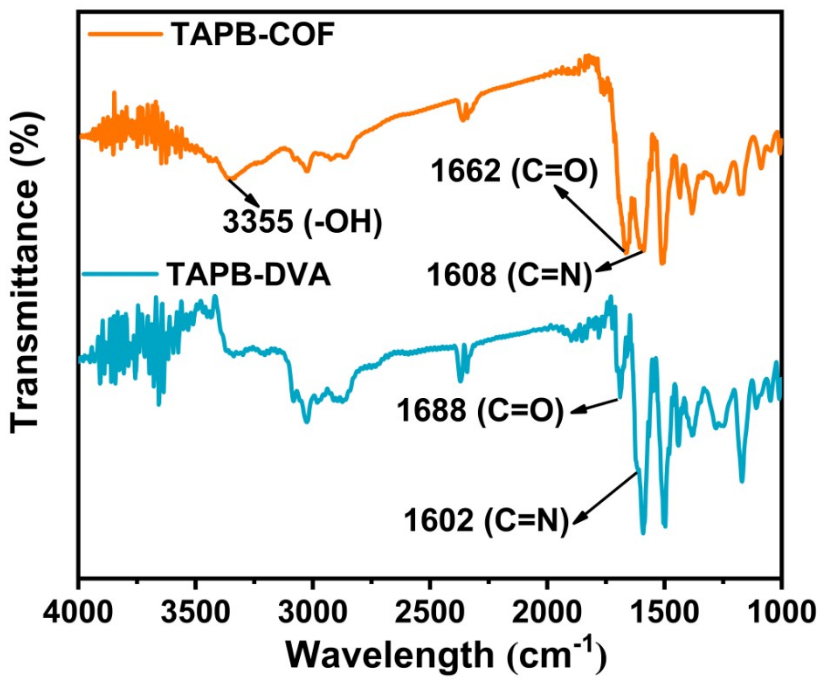

Fig. S5 FTIR spectra of TAPB-DVA, and TAPB-COF.

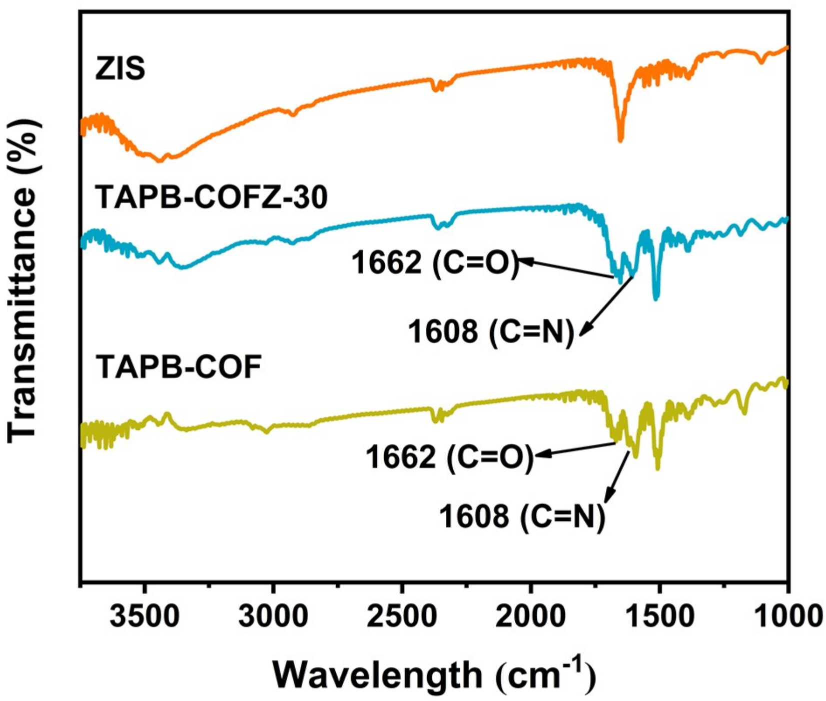

Fig. S6 FTIR spectra of ZIS, TAPB-COF, and TAPB-COFZ-30.

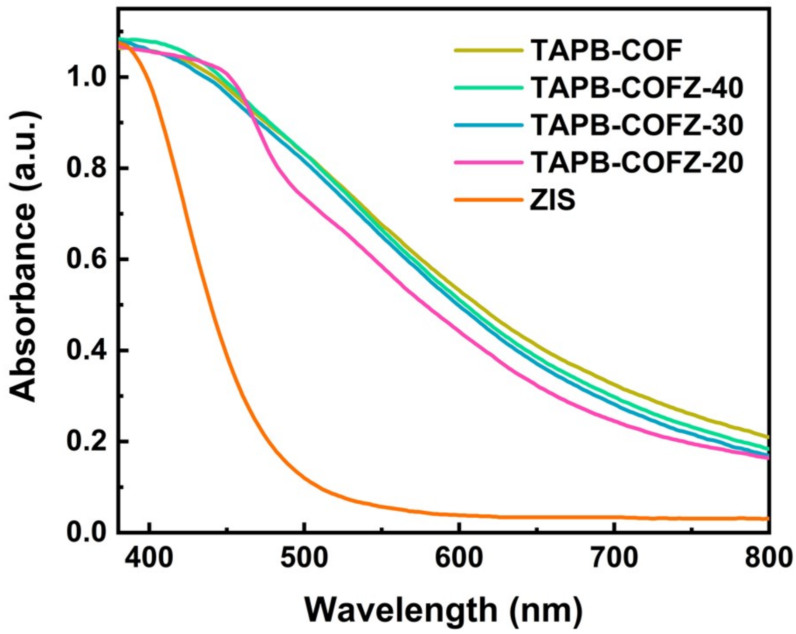

Fig. S7 UV-vis diffuse reflection spectra of different photocatalysts.

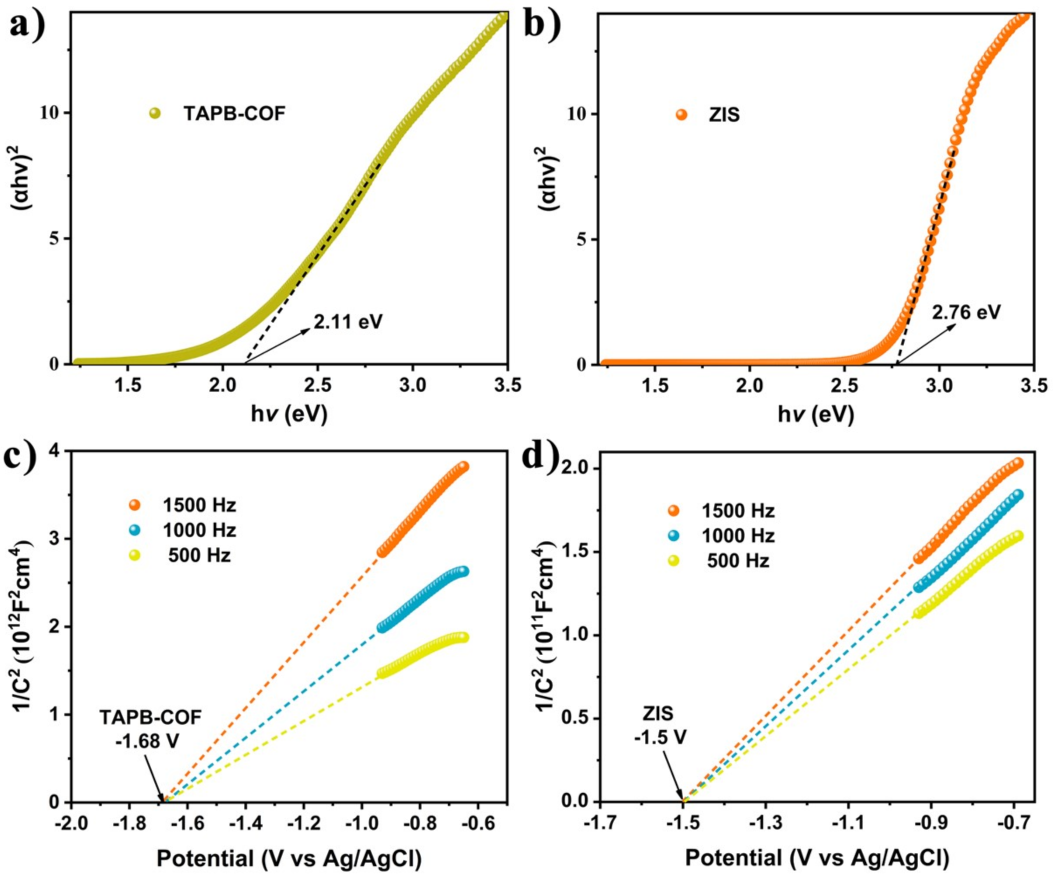

Fig. S8 a, b) Corresponding $(\alpha h\nu)^2$ versus hν plots and c, d) Mott–Schottky plots of TAPB-COF and ZIS.

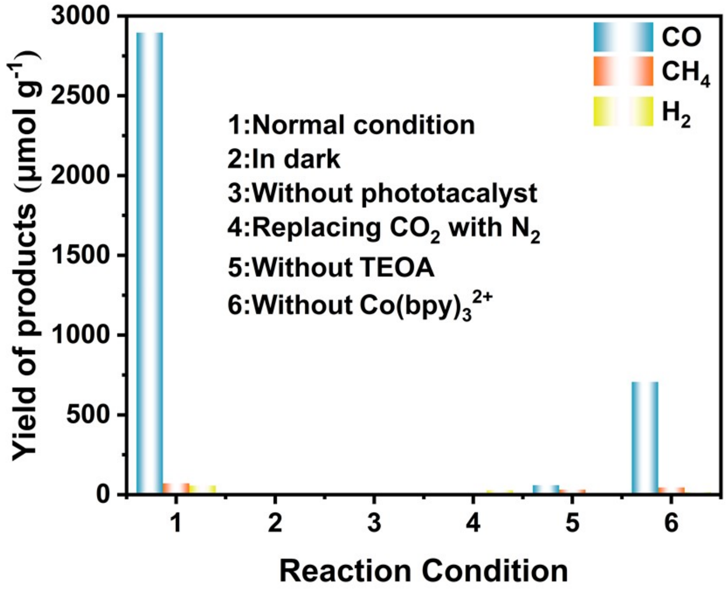

Fig. S9 Photocatalytic CO_2 reduction under different reaction conditions.

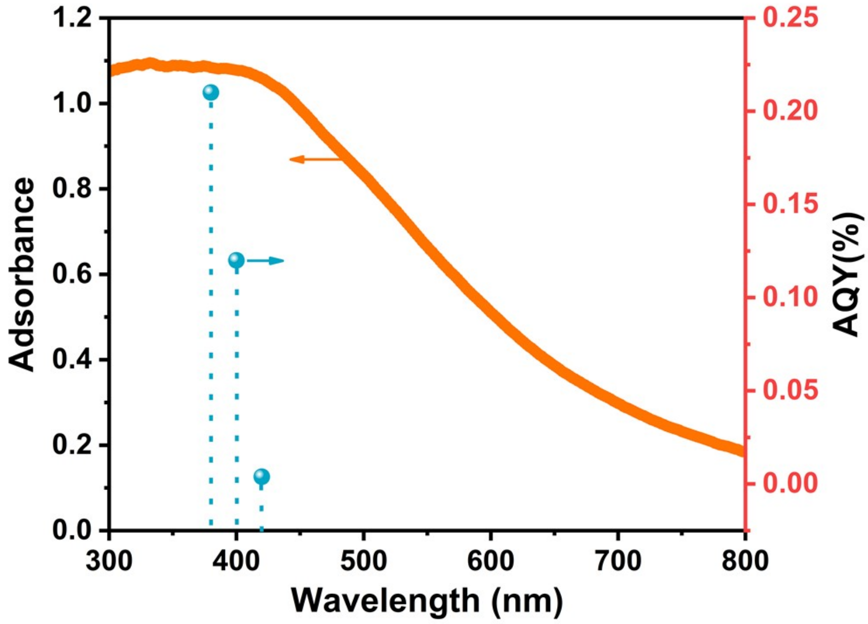

Fig. S10 Wavelength-dependent AQY% of TAPB-COFZ-30 photocatalyst under different monochromatic light irradiation (380 nm, 400 nm, 420 nm).

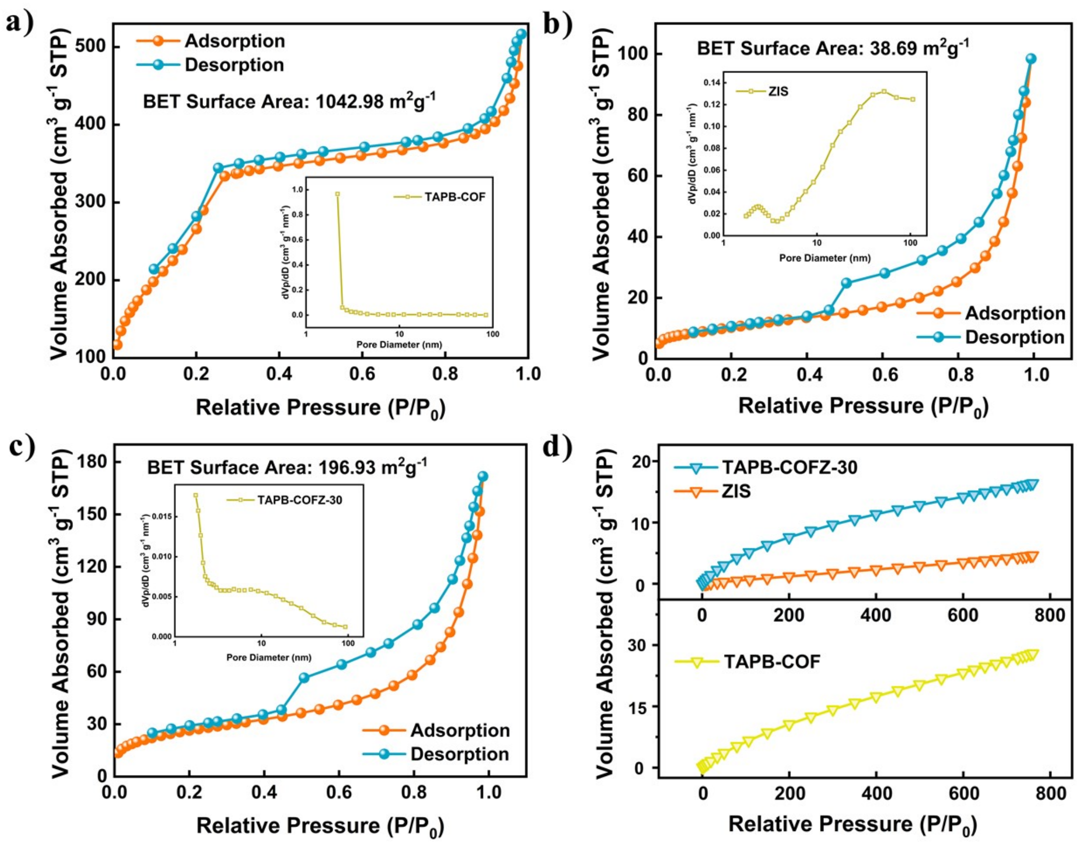

Fig. S11 a-c) Nitrogen adsorption for TAPB-COF, ZIS, and TAPB-COFZ-30. d) CO_2 adsorption of TAPB-COF, ZIS, and TAPB-COFZ-30.

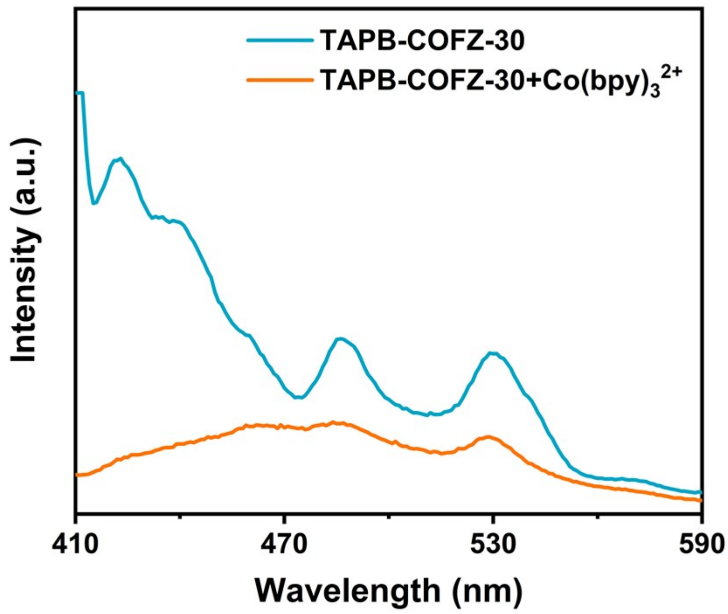

Fig. S12 Steady-state PL spectra of TAPB-COFZ-30 and TAPB-COFZ-30/$Co(bpy)_3^{2+}$ hybrid in the reaction mixture.

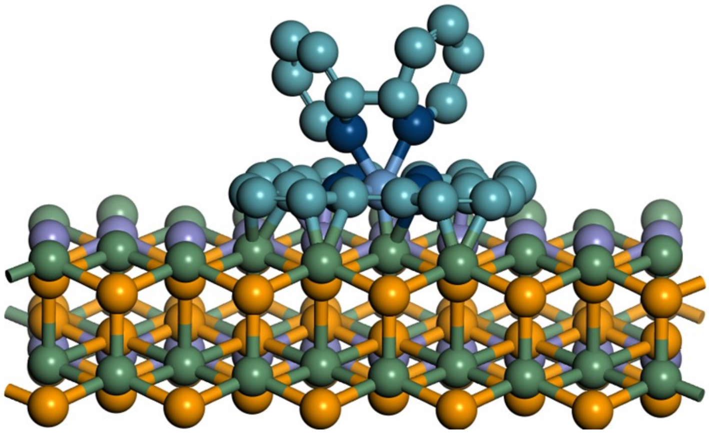

Fig. S13 Illustration of $Co(bpy)_3^{2+}$ adsorption on ZIS surface (E_{ads} = -3.43 eV).

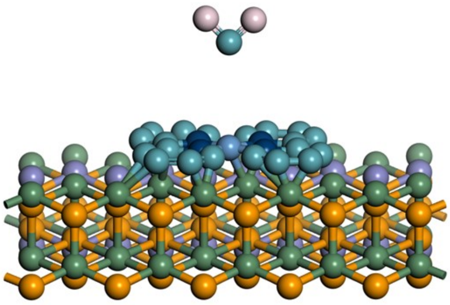

Fig. S14 Structural model of Gibbs free energy calculations on ZIS surface [CO_2(g)].

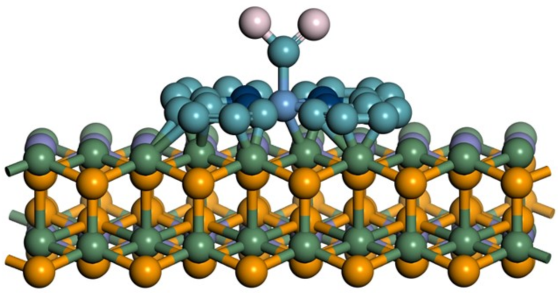

Fig. S15 Structural model of Gibbs free energy calculations on ZIS surface (*+CO_2).

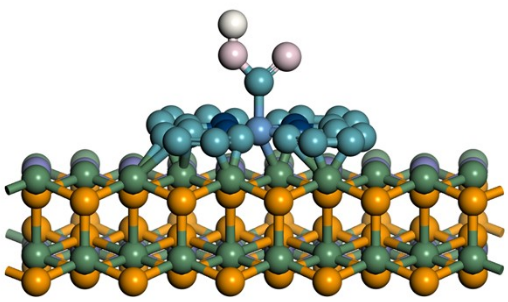

Fig. S16 Structural model of Gibbs free energy calculations on ZIS surface (*COOH).

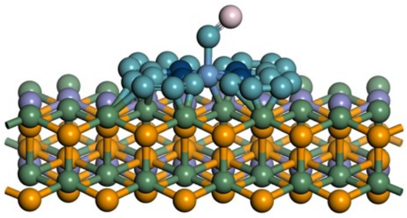

Fig. S17 Structural model of Gibbs free energy calculations on ZIS surface (*CO).

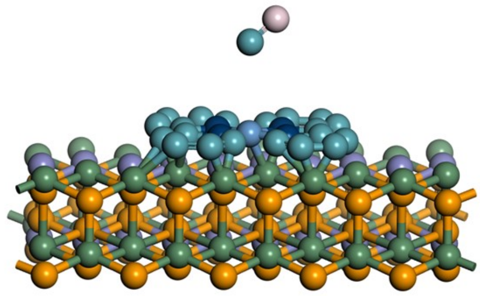

Fig. S18 Structural model of Gibbs free energy calculations on ZIS surface [*+CO(g)].

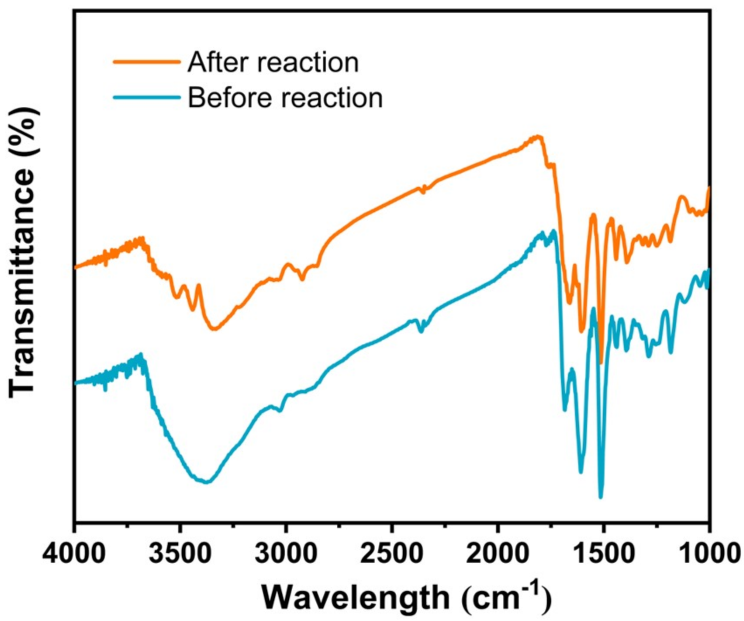

Fig. S19 FTIR spectra of TAPB-COFZ-30 before and after reaction.

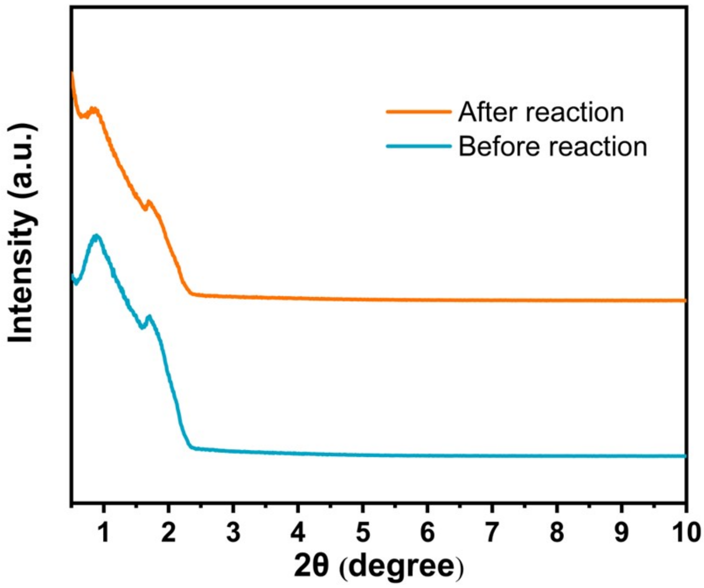

Fig. S20 PXRD pattern of TAPB-COFZ-30 before and after reaction (0.5-10°).

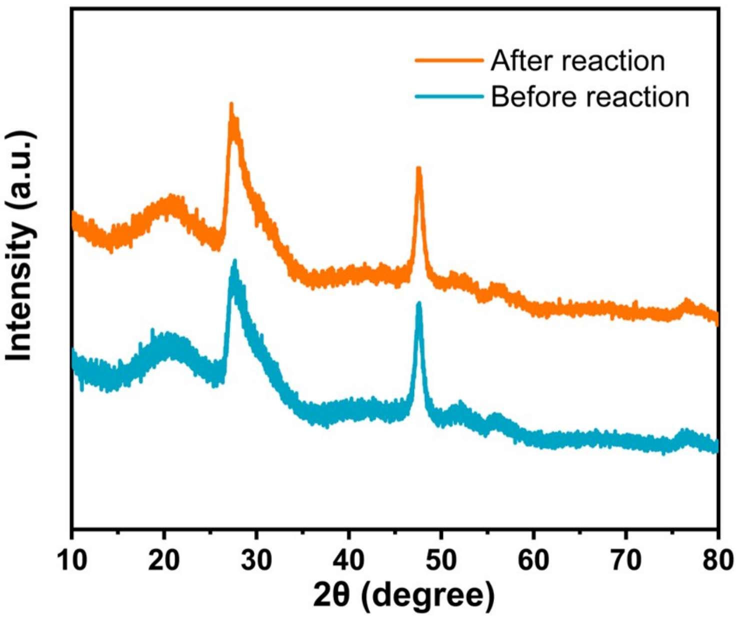

Fig. S21 PXRD pattern of TAPB-COFZ-30 before and after reaction (10-80°).

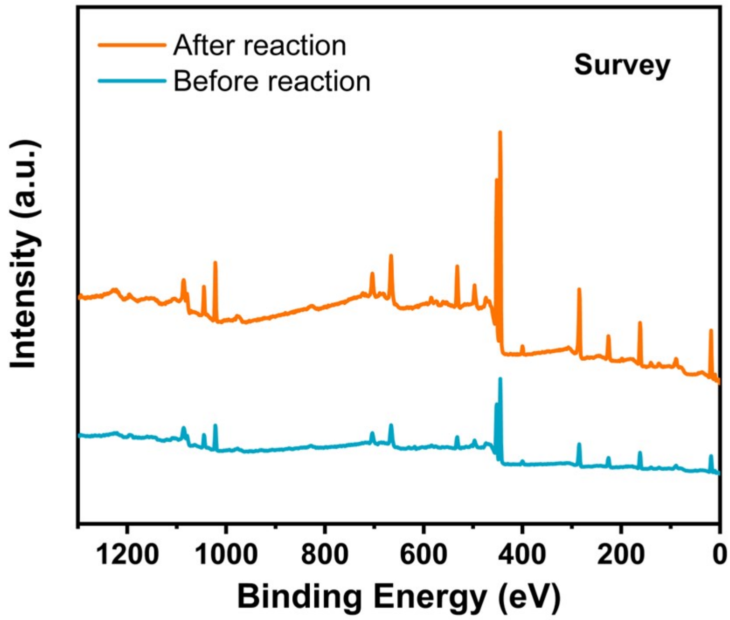

Fig. S22 XPS survey spectra of TAPB-COFZ-30 before and after reaction.

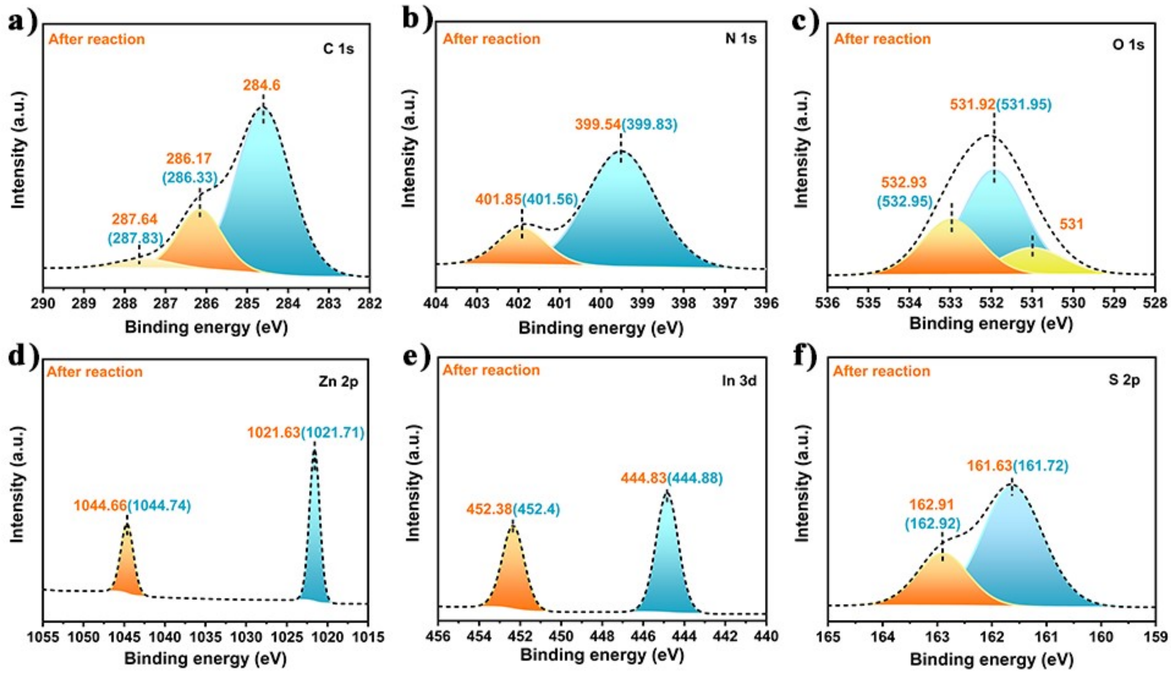

Fig. S23 High-resolution XPS spectra of TAPB-COFZ-30 after reaction: a) C 1s, b) N 1s, c) O 1s, d) Zn 2p, e) In 3d, and f) S 2p (the blue font is before reaction).

2. Summary Tables

Table S1. Light intensity and wavelength under different tests.

Test item	λ (nm)	light intensity (mW/cm^2)
Performance test	≥ 320	890
AQY	380	114.97
AQY	400	119.43
AQY	420	112.42

Table S2. Summary of photocatalytic CO_2 reduction performances of different catalysts after irradiation for 4 h.

Photocatalyst	Yield (CO) /μmol g^{-1}	Yield (CH_4) /μmol g^{-1}	Yield (H_2) /μmol g^{-1}
ZIS	466.63	34.61	81.46
TAPB-COF	87.42	0	26.84
TAPB-COFZ-20	1116.88	35.52	11.48
TAPB-COFZ-30	2895.94	71.48	56.91
TAPB-COFZ-40	856.90	15.9	40.81

$$\text{Selectivity of CO (\%)} = \frac{R(CO)}{R(CO) + R(CH_4) + R(H_2)} \times 100\%$$

Where R(CO), R(CH_4) and R(H_2) are the generation rates of CO, CH_4 and H_2.

Table S3. Comparison of photocatalytic CO_2 reduction performance with recently reported photocatalysts.

Photocatalyst	Reaction system	Mass (mg)	Light source	Main Products (μmol g^{-1} h^{-1})	AQY (%)	Ref.
$ZnIn_2S_4$/MOF-808	gas-solid system	50	300W Xe lamp	**CO:8.21**	n.d.	1

$Co_9S_8@Cd_{0.8}Zn_{0.2}S$-DETA	H_2O/MeCN/TEOA	15	300W Xe lamp ($\lambda \geq 420$ nm)	**CO:4673**	9.45 (420 nm)	2
BIO-LOV2	gas-solid system	20	300W Xe lamp	**CO:17.33**	0.34 (365 nm)	3
STAO/TiO_2	gas-solid system	2.5	300W Xe lamp	**CO: 182.1**	0.36 (380 nm)	4
viCOF-bpy-Re	gas-solid system	10	300W Xe lamp ($\lambda \geq 420$ nm)	**CO: 190.6**	1.08 (400 nm)	5
Mo-COF	gas-solid system	10	300W Xe lamp ($\lambda \geq 420$ nm)	**CO: 6.19** C_2H_4:3.57 CH_4:1.08	n.d.	6
AuNPS/ZIS	H_2O/MeCN/TEOA	5	300W Xe lamp ($\lambda \geq 420$ nm)	**CO: 366** CH_4:130	0.12 (450 nm)	7
CdS@CTF-HUST-1	H_2O/TEOA	10	300W Xe lamp	**CO:168.77**	2.34 (400 nm)	8
CdS@COF	H_2O/MeCN	5	300W Xe lamp ($\lambda \geq 420$ nm)	**CO: 507**	0.21 (420 nm)	9
COF-RuBpy-Co	MeCN/TEOA	5	300W Xe lamp ($\lambda \geq 420$ nm)	**CO: 547**	n.d.	10
C/CdS@$ZnIn_2S_4$	H_2O	20	300W Xe lamp (780 nm $\geq \lambda \geq$ 420 nm)	**CO:115.4**	n.d.	11
SnS_2/S-CTFs	H_2O/TEOA	20	300W Xe lamp ($\lambda \geq 420$ nm)	**CO: 123.6** CH_4: 43.4	n.d.	12
TAPB-COFZ-30	**H_2O/MeCN/TEOA**	**5**	**300W Xe lamp**	**CO:723.985**	**0.21 (380 nm)**	**This work**

Notes: MeCN = acetonitrile; TEOA = triethanolamine; n.d.= not detected

Table S4. The fitting parameters of the TRPL spectra of TAPB-COFZ-30 and ZIS.

Sample	**A_1 (%)**	**τ_1 (ns)**	**A_2 (%)**	**τ_2 (ns)**	**Ave.τ (ns)**
TAPB-COFZ-	29.37	0.34	70.63	2.29	2.17

30					
ZIS	22.58	0.19	77.42	1.73	1.68

References

1 M. Song, X. Song, X. Liu, W. Zhou, P. Huo, *Chinese J. Catal.* 2023, **51**, 180-192.

2 B. Su, M. Zheng, W. Lin, X.F. Lu, D. Luan, S. Wang, X.W. Lou, *Adv. Energy Mater.* 2023, **13**, 2203290.

3 F. Chen, Z. Ma, L. Ye, T. Ma, T. Zhang, Y. Zhang, H. Huang, *Adv. Mater.* 2020, **32**, 1908350.

4 Y. Feng, C. Wang, P. Cui, C. Li, B. Zhang, L. Gan, S. Zhang, X. Zhang, X. Zhou, Z. Sun, K. Wang, Y. Duan, H. Li, K. Zhou, H. Huang, A. Li, C. Zhuang, L. Wang, Z. Zhang, X. Han, *Adv. Mater.* 2022, **34,** 2109074.

5 Y.Z. Cheng, W. Ji, P.Y. Hao, X.H. Qi, X. Wu, X.M. Dou, X.Y. Bian, D. Jiang, F.T. Li, X.F. Liu, D.H. Yang, X. Ding, B.H. Han, *Angew. Chem. Int. Ed.* 2023, **62,** e202308523.

6 M. Kou, W. Liu, Y. Wang, J. Huang, Y. Chen, Y. Zhou, Y. Chen, M. Ma, K. Lei, H. Xie, P.K. Wong, L. Ye, *Appl. Catal. B-Environ. Energy* 2021, 291, 120146.

7 S. Si, H. Shou, Y. Mao, X. Bao, G. Zhai, K. Song, Z. Wang, P. Wang, Y. Liu, Z. Zheng, Y. Dai, L. Song, B. Huang, H. Cheng, *Angew. Chem. Int. Ed.* 2022, **61**, e202209446

8 G. Zhang, X. Li, D. Chen, N. Li, Q. Xu, H. Li, J. Lu, *Adv. Funct. Mater.* 2023, **33**, 2308553.

9 L. Zou, R. Sa, H. Zhong, H. Lv, X. Wang, R. Wang, *ACS Catal.* 2022, **12**, 3550-3557.

10 L.-J. Gong, L.-Y. Liu, S.-S. Zhao, S.-L. Yang, D.-H. Si, Q.-J. Wu, Q. Wu, Y.-B. Huang, R. Cao, *Chem. Eng. J.* 2023, **458**, 141360.

11 X. Zhang, P. Wang, X. Lv, X. Niu, X. Lin, S. Zhong, D. Wang, H. Lin, J. Chen, S. Bai, *ACS Catal.* 2022, **12**, 2569-2580.

12 S. Guo, P. Yang, Y. Zhao, X. Yu, Y. Wu, H. Zhang, B. Yu, B. Han, M.W. George, Z. Liu, *ChemSusChem* 2020, **13**, 6278-6283.